Master ASEP
Manuel Pichardo Marcano

MUSE integral field unit observations of the compact objects in the globular cluster NGC 6397

Advisor : Dr. Natalie Webb, IRAP.

Abstract

Globular clusters are very old groups of stars. Due to their age and the gravitational interactions dominating the dynamics of the clusters, they are home to a significant fraction of compact binaries. The formation and evolution of these kinds of binaries is still not completely understood. Of special interest is the globular cluster NGC 6397 as it is the closest core collapsed cluster and has therefore been extensively studied with instruments like Chandra, Hubble Space Telescope, and more recently in the optical with the Multi Unit Spectroscopic Explorer (MUSE), installed on the Very Large Telescope (VLT). Integral field spectrographs, like MUSE, have many advantages compared to traditional long slit spectroscopy, as spectra are obtained for every pixel and thus every object in the large field of view ($1'$ x $1'$). Here we present analysis of the compact binary population in NGC 6397 taken with MUSE. The goal is to further understand the characteristics of the proposed bimodal population of cataclysmic variables in the cluster, which have been suggested to be of primordial and dynamically formed origin. Spectral analysis will allow us to examine the origin of these two populations.

Contents

Chapter 1: Introduction

1.1 Location, Location, Location

Important in real estate, but also seems to be an important factor to take into account when studying compact objects in binary systems. It seems that, like with people, where you were born plays a role on your evolution. This seems to be true for cataclysmic variables (CVs), the kind of compact binary system that we will explore in more detail in the present work. Our goal is to try to understand the formation of these kind of systems when they are formed in a crowded and high density environment (like in a cluster of stars), and when you give them enough time to evolve and interact with other stars (like in a globular cluster).

Now that we have defined our broad goal let's take a step back and explore in more detail what are compact objects, their different types, and the different ways they can interact with each other and other types of stars (Sec. 1.2). That section will lead us to the discussion of where and how we expect to find them, and what can we learn by studying them in the different environment where they form (sections 1.4).

1.2 Compact Objects or Stellar remnants

Compact object, as their name suggest, are very massive and dense objects formed from the remains of a dying stars; hence their other name, 'stellar remnants'. They come in three main flavors, each following a different formation mechanism that is mainly determined by the mass of the progenitor star (ref.). The different types are neutron stars (NS), black holes (BH), and white dwarfs (WD). Besides these three, other possible exotic types of stars have been proposed; including quark stars, boson stars, and Thorne-Zytkow objects. These will not be discussed in this work as there is still a lack of observational evidence concerning their existence. The reader is refer to the following references to discover more about these particular kind of proposed stars. (Find references for exotic stars).

On the three confirmed compact objects (neutron stars, white dwarfs and black holes), we will focus on the first two (NS and WD). They below to a class of object called "degenerate objects". These are object for which the supporting force comes from the degeneracy pressure of fermions[1]. In the case of a white dwarf the pressure is provided by the degenerate electron gas (Fowler, 1926), and for a neutron stars, clearly, the neutrons cause the repulsive pressure (ref).

The next subsection will list some of the characteristic for NS, and WD (both when they are found in isolation (sec 1.2.1 and 1.2.2) or in a binary system sec 1.3). Black holes will be briefly discussed for the sake of completeness.

1.2.1 White Dwarfs

White dwarfs are the most common end product in the evolution of stars. Around 90% will evolve to become one (Koester & Weidermann, 1980). This includes all main sequence stars [2] (MS) with a

[1]Fermions are particles with half-integer spin. They follow the Fermi-Dirac statistics, thus obey the Pauli exclusion principle. The consequence of the exclusion principle is that two fermions cannot occupy the same quantum state. This is the origin of the degeneracy pressure.

[2]Main sequence stars are those that are burning hydrogen in their cores.

mass between 0.6 and 8 $M_\odot$ (Koester & Chanmugam, 1990). The resulting white dwarf will have a mass between 0.3 and 1.4 $M_\odot$ (Prada Moroni & Straniero, 2009; Chandrasekhar, 1931), the average mass being ~ 0.7 $M_\odot$ (Koester & Chanmugam, 1990). All this mass is contained in a radius of about ~ 0.01 $R_\odot$ (Kepler & Bradley, 1995). This are average values, but the mass-radius relation for a white dwarf is plotted in fig 1.2. If we take the mean values mentioned before this gives a mean density of 10^9 kg/m^3 . This mass-radius relation will be composition dependent and it depends, for example, on the element dominiating the atmosphere composition (Hamada & Salpeter, 1961). About 80% of all white dwarfs have hydrogen-dominated atmospheres (spectral type DA), but there exists a second class where helium dominates the atmosphere composition (spectral types D0, DB, DC, DZ and DQ)(Wickramasinghe & Ferrario, 2000; Koester & Chanmugam, 1990). White dwarfs are also known to be magnetic. Surface magnetism ranges from about 10^5 to 10^9 G (Suh & Mathews, 2000). Isolated magnetic whit dwarfs represent $\sim 5\%$ of all WDs. See Wickramasinghe & Ferrario (2000) for a review on magnetism in WDs and for more details on the physics of white dwarfs the reader is referred to Koester & Chanmugam (1990) and Kepler & Bradley (1995).

1.2.2 Neutron Stars

Neutron stars, first proposed in 1934 by Baade and Zwicky, are stars where the sustaining force against gravity comes from the degeneracy pressure between neutrons (Baade & Zwicky, 1934). These stars are produced from the gravitational collapse of a massive star ($>$ 8 $M_\odot$)(ref for mass range) at the end of its life. The type II supernova produced by this collapse, leaves behind a dense and massive core. A core of ~ 12 kilometers in radius (ref), but up to ~ 2 $M_\odot$ (this limit being model dependent. See (Lattimer & Prakash, 2007)). For comparison with white dwarf a sample mass-radius relation for a NS (red) is plotted along with that of a white dwarf (blue) in fig 1.2. Like WDs, neutron stars are also know to show magnetism. They have an average magnetic field strength of $< B > \sim 10^{14}$ G (Beskin et al., 2015). There also exist some neutron stars with unusually high strong magnetic fields (B $\sim 10^{14} - 10^{15}$ G) and are called "magnetars" (Duncan & Thompson, 1992). For a review on magnetic fields in neutron stars see Reisenegger (2005).

Neutron stars are mainly composed of neutrons and a thin atmosphere of a few cm of hydrogen or helium (ref for NS atmosphere models). We have come a long way since the first proposition of their existence, but there is still a lot of uncertainty concerning their interiors and a lot of existing conflicting models (Lattimer & Prakash, 2007). Since we have had observational evidence on their existence (ref PSR B1919+21) efforts have been done to constrain the different models. Figure 1.1 shows a visual summary of some of the different models proposed. There are many ways that we can observationally constrain these models, spectroscopy being one of them.

1.2.3 Black Holes

Black holes are the fate of collapsing matter when no force, including the degeneracy pressure of neutrons, is not enough to repel gravitational attraction. Black holes, like neutron stars and white dwarfs, can be the result of the collapse of a single main sequence star. Stars with an initial mass $\gtrsim 20$ can end up as a black hole (Heger et al., 2003), but the initial mass is not the only factor that comes into play. For example, the formation of the black hole will depend also on the metallicity of the star as well as the initial mass. See Heger et al. (2003) and (Brown et al., 2000) for details on the evolution of high mass stars and the different formation path leading to a black hole from a single collapse star.

To compare the physical characteristic of a black hole to other compact objects we can define the

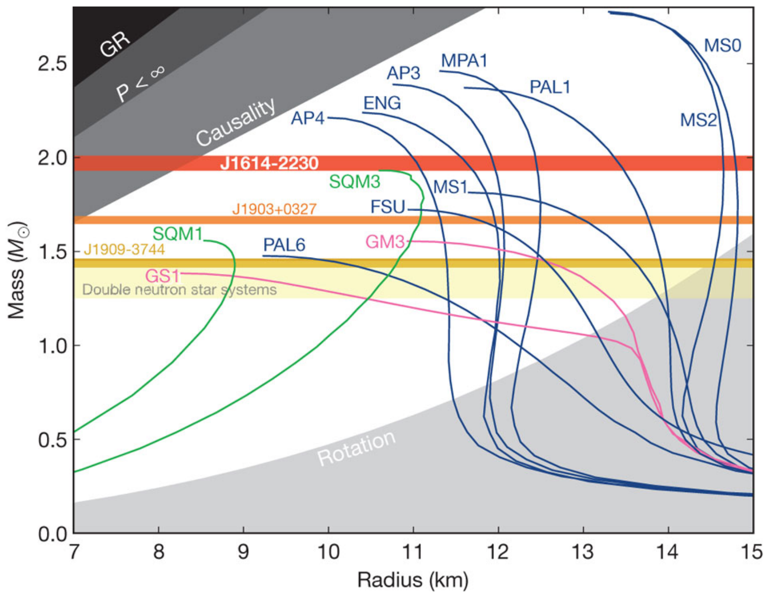

Figure 1.1: The plot shows non-rotating mass versus physical radius for several typical equation of states. Blue, nucleons; pink, nucleons plus exotic matter; green, strange quark matter from (doi:10.1038/nature09466)

gravitational radius or Schwarzschild radius of a black hole. This is the radius to which a given mass needs to be reduced to get a escape velocity equal to the speed of light. This translates to:

$$r = \frac{2MG}{c^2} \tag{1.1}$$

An estimate of the lowest mass of a black hole is the maximum possible mass for a neutron star, this is $\sim 3\mathrm{M}_\odot$ (Rhoades & Ruffini, 1974). With the formula above we can get a rough estimate on the size of a stellar mass black hole. A mass of 3 $\mathrm{M}_\odot$ and the formula above gives an equivalent Schwarzschild radius of about 9 km.

1.3 Compact Binaries

Compact binaries are those binaries where at least one of their components is a compact objects (WD, NS or BH). In this section we will start by discussing some of the basic concepts of binary evolution, follow by a discussion on mass exchange between binaries, and finished by looking in more detail some specific examples of compact binaries that are relevant to this study.

1.3.1 The Gravitational Potential

The total potential of a binary system is the sum of the gravitational and the rotational potential. To get an analytical solution we can assume a model in which the resulting disturbing potential is due to the presence of two point masses, M_1 (or the primary) and M_2 (also called the secondary). Moreover, we assume a co-rotating Cartesian reference frame (x,y,z) with origin at the primary M_1; whose x-axis is is in the direction joining the two point masses; and the z-axis is perpendicular to the orbital plane. The total potential at an arbitrary point P(x,y,z) then reads:

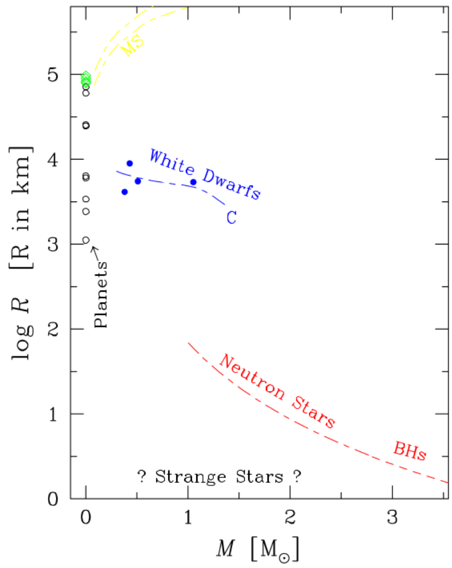

Figure 1.2: Mass-radius relation for different objects (de Boer & Seggewiss, 2008).

$$\Psi = -G\frac{\mathrm{M}_1}{\sqrt{x^2+y^2+z^2}} - G\frac{\mathrm{M}_2}{\sqrt{(R-x)^2+y^2+z^2}} - \frac{\omega^2}{2}\left[(x-\mu R)^2+y^2\right] \tag{1.2}$$

where G is the gravitational constant, R represents the separation between the point masses, and $\mu = \mathrm{M}_2/(\mathrm{M}_1+\mathrm{M}_2)$. We further assume that the binary orbit is Keplerian, thus the orbital frequency is given by:

$$\omega^2 = G\frac{\mathrm{M}_1+\mathrm{M}_2}{R^3} \tag{1.3}$$

Taking into the account the assumptions the surfaces generated by eq 1.2 are called *Roche Equipotential*[3]. Fig 1.4 such such equipotential surfaces (x,y plane). Of special interest are two regions on the graph:

- The inner Lagrangian point $\mathbf{L}_1$. This is where all the forces cancel out.
- Critical or **Roche lobe**. The surface that have the potential equal to the L_1 potential.

The Roche lobe has the property that inside the lobe of an object, any material will be gravitationally bound to that object. With these knowldege we can classify binary systems in three groups:

1. **Detached systems**. If the volumes of both components are significantly smaller than their Roche lobe.
2. **Semi-detached systems**. Where one of the components fills its Roche lobe.
3. **Contact systems**. Where both components appear to fill their respective Roche lobes.

[3]We are neglecting here the radiation pressure from the stars. For more details on Roche Potentials Including Radiation Effects see Schuerman (1972)

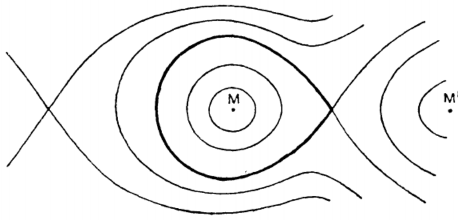

Figure 1.3: Geometry of the Roche surfaces. The Roche lobe is mark in bold font (Kopal, 1959).

This classification scheme was first suggested by (Kopal, 1955) and developed in detail in a comprehensive monograph in 1959 (Kopal, 1959).

1.3.2 Binary Evolution

In this work we are mostly interested in the formation of semi-detached compact binary systems. In this section we briefly explore a possible scenario for its formation.

These kind of systems can be formed from two previously detached MS stars binaries that evolve in different timescales due to their different mass. This can be seen noticing that the luminosity, L, indicates the rate of consumption of nuclear fuel; and the nuclear fuel repository is proportional to the mass, M. This gives us a rough estimates of the nuclear timescale of a star given by:

$$\tau \propto \frac{M 6 \times 10^{18} \text{ergs g}^{-1}}{L} \tag{1.4}$$

Where L is the luminosity, M is the mass, and 6×10^{18}ergs g^{-1} is the energy release fusing a gram of hydrogen to helium. Moreover, with the mass-luminosity relation $L/L_\odot = (M/M_\odot)^\alpha$, where $\alpha \gtrsim 3$ (ref. missing), we can conclude that in a system starting with two detached main sequence stars, the more massive one will leave faster the main sequence and finished as a compact object (depending on its mass). This will leave a binary system with a compact object and a evolved main sequence star. The old main sequence star in the binary as it continues evolves will expand and fill its Roche lobe, allowing for accretion into the compact object to happen. The process is more complex and, among other things, depends on the initial mass of both stars and initial binary separation. For example, a binary system starting with a 2 $M_\odot$ and a 1 $M_\odot$ star can produce a white dwarf accreating from a late-type main sequence star (Kippenhahn et al., 1967; De Loore & Doom, 1992). A system starting with a 15 $M_\odot$ and 2 $M_\odot$ will become a neutron star accreting from a low mass main sequence star (Heuvel & J, 1976). In the case of starting masses of 20 $M_\odot$ + 8 $M_\odot$ this can produce a neutron star (or black hole) accreting from a high mass main sequence star (Heuvel & J, 1976). The details on the evolution of close binaries can be found in Postnov & Yungelson (2014).and (de Boer & Seggewiss, 2008)

In the next section we will see in some detail how the accretion can take place once the compact binary is formed due to stellar evolution of their constituents.

1.3.3 Accretion

As mentioned before if one of the binaries fills its Roche lobe, material can flow via the L_1 point to the other star. This is what constitutes a semi-detached binary system. It would be a semi-detached compact binary if at least one is a compact object. Here we look in more detail the nature of the accretion in such a system where a compact object (primary) accreates from a main sequence star via Roche lobe overflow.

In the Roche overflow scenario we have incoming gas from the secondary star. After it passes thought the L_1 point we assume a ballistic behaviour completely governed by the gravitational potential of the compact object. This is justified by the fact showed by Lubow & Shu (1975) that the stream is supersonic and we can ignore pressure. We can also assume that the incoming speed must be small. This is safe to assume if the accretion is due solely to overflow of the lobe and thus the velocity is in the order of the sound speed at the atmosphere of the secondary star. This speed ($\sim$ 10km/s reference missin) is much slower than the orbital speed of the binaries, and lower than the velocities acquire during the fall. This simplification means that we can treat the Roche lobe as a zero velocity surface. Meaning that the motion of the gas can be approximated as the trajectory of a test particle release from rest with an initial angular momentum from L_1. This creates an elliptical orbit of the stream around the primary star (fig 1.4 a). As the gas flow continues it will impact itself. This causes the flow to modify its orbit to that of the lowest energy at an specific angular momentum (we assume angular momentum is conserve). Of course the orbit of lowest energy at a given angular momentum is a circular one (see fig 1.4 b). This creates a ring around the compact object. We can estimate the radius of this ring by again invoking the assumption that no angular momentum is loss in the process. The angular momentum at L_1 would be given by R_{L1} V_{orbit} (where R_{L1} is the distance from the secondary to L_1). Knowing that $\omega = (2\pi)/\text{Period}$ and equating the angular momentum at L_1 to the angular momentum of a Keplerian orbit at R_{ring} we get:

$$\frac{R_{ring}}{R} = \left(\frac{\mathrm{R}_{L1}}{R}\right)^{\frac{1}{4}} (1+q) \tag{1.5}$$

where I used eq 1.3 to simply the answer by canceling some constants. This is called the *circulation radius*. After a ring is formed (fig 1.4 b), as first indicated in Lynden-Bell & Pringle (1974), any viscous processes will cause the ring to spreads to conserve angular momentum (fig 1.4 d) The nature of these viscous torque won't be discussed here. For a review on the topic see Frank et al. (2002) and Verbunt (1982). It is only left to say that Roche lobe overflow is not the only type of accretion, for example wind accretion. In this work, unless otherwise stated, accretion will mean accretion by Roche lobe overflow. See the references cited above for more detail on other type of accretion.

Now that we studied briefly accretion and see how it can happen in semi-attached binaries, in the next section we will discuss two specific examples of this happening. One where the accretion is onto a white dwarf (Cataclysmic Variable), and the other where the accretion is onto a neutron star or a black hole (X-Ray binaries).

1.3.4 Cataclysmic Variables (CVs)

Cataclysmic variables are semi-detached binary system comprised of a white dwarf (primary star) and typically a low mass main sequence star with a typical period in the range of 1-10 hrs (ref for period). CVs are generally classified into two groups. Magnetic CVs and nonmagnetic CVs (B $<$ 0.01 MG). Magnetic CVs constitute about 25% of the CV population (Balman, 2012).

CVs can be observed in many wavelengths. This includes radio observation of jets (Körding et al., 2008; Coppejans et al., 2015), optical and UV observation of the accretion disks Kinney (1994), and X-rays ($\sim 0.5 - 2.5keV$) from the infalling plasma onto the white dwarfs (Kuulkers et al., 2006). As

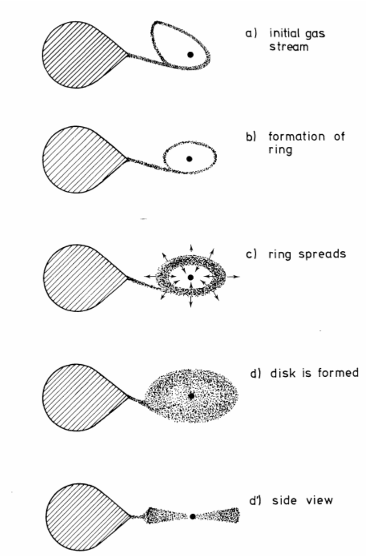

Figure 1.4: Schematic illustration of the formation of an accretion disk around a compact binary (Verbunt, 1982).

their name suggest these are very variable systems (specially the nonmagnetic CVS). These variabilities are due either by instability on the accretion disk, referred to as dwarf nova (Osaki, 1974), or unstable burning of hydrogen at their surface, called nova (Starrfield et al., 2016). We will discuss in some detail the outburst caused by these instabilities, and the nature of the magnetic CVs by presenting the classification of CVs and exploring the taxonomy of these objects.

1.3.4.1 Classical Novae (CN)

When the surface of an accreting white dwarf becomes hot enough ($\sim \times 10^8$ K Starrfield et al. (2016)), nuclear fusion can take place and a thermonuclear runaway happens. This creates a violent explosion capable of ejecting material (mean mass of $\sim 2 \times 10^{-4} M_\odot$) at high velocities ($\sim 10^2 - 10^3$ km s^{-1}) (Gehrz et al., 1998; Shara, 1989). These outburst are fairly easy to detect since they cause a substantial increase in brightness (typically $\sim$ 12 magnitudes Shara (1989)). A CV observed erupting in such a way is classified as a *classical nova (CN).* Classical novae are seen to erupt only one. If a previously recognized CN erupts again as a CN they are called recurrent novae.

1.3.4.2 Dwarf Novae (DN)

A dwarf nova outburst is caused by instabilities in the accretion disk. This is predicted to happened in non-magnetic CVs with low accretion rates (Osaki, 1974). CVs that show these outbursts are classified as dwarf nova. The outburst from a dwarf nova is not as violent as the one from a classical novae. The magnitude change is only of about 2-5 , and no material is ejected. They also, unlike classical novae, are periodic in nature on times scales of weeks to years depending mainly on the accretion rate (Shara, 1989). Probably the best know example of a dwarf nova is the variable star SS Cygni Cannizzo & Mattei (1998).

1.3.4.3 Novae-like (NL)

Another classification of white dwarfs is the novae-like. They are CVs that seem to have stable accretion, thus not undergoing dwarf novae outburst and having a bright stable disk. They represent the 'non-eruptive' CVs.

1.3.4.4 Polars

Polars are CVs with a strong magnetic field. The value of the magnetic field is usually between 20 MG to 230 MG (Balman, 2012). The field in polars is so strong that it couples to the field of the donor and forces the WD to corotate with the binary. The presence of the strong magnetic field also disrupt the accretion disk. In the case of Polars the accretion flow is redicted so it takes place at the magnetic pole guided by the magnetic field lines. This causes X-ray radiation and strongly polarized cyclotron radiation from IR to UV wavelengths (Cropper, 1990). This polarized emmision is the reason for the name Polars (Krzeminski & Serkowski, 1977). The polarization was the first clue on the magnetic nature of these type of systems. It was first discovered for AM Herculis (AM Her), now the prototype polar CV (Tapia (1977)). Polar systems are often referred to as AM Her-like system. This kind of systems represent 63% of the magnetic CV population (Balman, 2012).

1.3.4.5 Intermediate Polars (IPs)

Intermediate polars are the second kind of magnetic CVs. In this type the magnetic field is weaker ($\sim 1-20MG$). The weaker strength of the magnetic fields means that the accretion disk is not entirely dominated by the magnetic field, and the system is asynchronous, so the WD does not corotate with the binary. This kind of systems represent 37% of the magnetic CV population (Balman, 2012). An extensively studied member of this class is DQ Her. DQ Her is somethings refer as a subclass of IPs (IPs with period $\lesssim$ 120 s), or even as a synonym for IP (Patterson, 1994; Warner, 2003).

Should I include AM CVn?

1.3.5 X-Ray binaries

X-Ray binaries are a subclass of compact binaries where the accretor is either a neutron star or a black hole. They can be classified into two regimes depending on the type of the donor star. If the donor or secondary is a late-type star it is called, Low-mass X-ray binary; if it is an early-type star they are called high-mass X-ray binary.

1.3.5.1 Low-mass X-Ray Binaries

Low-mass x-ray binaries (LXMBs) are Roche-lobe overflow binary stars consisting of a neutron star or a black holes accreating from a low-mass ($\lesssim 1.5\mathrm{M}_\odot$) donor. The donor can be a main sequence star or even a white dwarf (Tauris & van den Heuvel, 2006).

In the case of a LMXB, since the accretor (NS or BH) has a higher mass than the white dwarf in a CV, the energy release in the accretion process is higher. This means that we get more powerful X-ray radiation from LMXB (up to $\sim 10\mathrm{k}eV$) (Tauris & van den Heuvel, 2006). The period can range from 11 minutes to 17 days, and like CVs they can show magnetism ($\sim 10^9 \sim 10^{11}$G). (Do I use ibid. or cite again?).

1.3.5.2 High-mass X-Ray Binaries

High-mass X-ray binaries (HMXB) are the second class of X-ray binaries. In the case of an HMXB the donor star is a young early-type main sequence star. This usually means a O or B spectral type with a mass $> 10\mathrm{M}_{\odot}$ (Tauris & van den Heuvel, 2006). Contrary to the LMXB the accretion is not entirely due to Roche overflow, it can be due to the high velocity winds produced by the donor star. And also unlike the LMXB this systems tend to show stronger magnetic fields and stronger X-ray radiation (ibid.)

1.3.6 The secondary stars

1.4 Globular Clusters

Globular clusters (GCs) are very old and dense gravitationally bound group of stars. Their age is generally around 10 Gyr (Meylan & Heggie, 1997) and typically contain $\sim 10^6$ stars (Knigge, 2012). Due to their age we expect to find compact objects, and the high density environment is ideal for the formation of compact binaries. The search for these compact binaries have been fructiferous leading to the detection of X-ray binaries (()citation) and Cataclysmic Variables ((**?**)itation) in several globular clusters. But still the formation and evolution of these kinds of binaries is still not completely understood, and many uncertainties remain. Of special interest for this project are the cataclysmic variables in globular clusters. In the next subsection we will make a brief overview on the current knowledge on the subject and state the current open questions that we mean to address in this project.

1.4.1 CVs in Globular clusters

Cataclysmic Variables are tracers of the dynamical evolution in globular clusters. Their number and spatial distribution can give us a clue on the past of the globular cluster, and help us constraint models of stellar and dynamical evolution. CVs are expected to be the most abundant compact binary based on the fact that white dwarf is the most common fate of stars. Theoretical modeling predicts $\sim 100 CVs$ in a given GC (Ivanova et al., 2006). They are expected to form two distinctive groups based on their formation mechanism, primordial CVs and dynamically formed CVs (Hut et al., 1992). Primordial are those CVs that formed from primordial binaries that didn't get destroyed through a physical collision in the cluster.The dynamically formed CVs are those formed via dynamical encounters with other members in the cluster. This includes tidal capture, exchange interactions and collision events. For example a dynamically formed CV can formed thought the tidal capture of an MS by a WD, or by a system resulting from the collisions between a red giant and a MS star (Ivanova et al., 2006).

The two expected formation mechanism clearly raises the question **Where are all the primordial CVs?**. The number can be theoretically predicted ($\sim 37\%$ of all CVs in a GC (Ivanova et al., 2006)), but we need observational evidence to constraint the theoretical models. This still remains the case. The dense environment in which they form and the possibility that CVs are formed through dynamical interaction can result in a differentiation of the binary population from the galactic field population. For example, the result of these dynamical processes is that in the dense cores of GCs, binaries are strongly depleted and their period distribution is expected to be different from that of a field population (Ivanova et al., 2005). So the questions becomes, **What is the period distribution of CVs in Globlular Clusters**. In the galactic field the period distribution have been well studied. The period of CVs in the field is governed by magnetic braking ($\mathrm{P}_{orb} \gtrsim 3$h), and gravitational radiation ($\mathrm{P}_{orb} \lesssim 2h$) (ref for period gap). The period distribution in GC is still not well understood mainly due to lack of observational data. There are only 15 CVs with know periods from a small sample of 5 globular clusters (Should I cite all studies or can I cite a paper with all of them like Knigge (2012)). Another difference between fields and GC CVs that have been proposed is that CVs in GCs tend to be primarily magnetic in nature (Grindlay, 1999). This will explain the lack of observed dwarf novae outburst in CVs (ref) and the high X-ray luminosity of GC CVs, compared to fields CVs (Verbunt et al., 1997). However data is scarce to support that argument and the questions remain: **Are globular clusters in CVs mainly magnetic in nature and where are all the dwarf novae?**

With the questions mentioned above in mind, in this project we studied the population of Cataclysmic Variables in an specific nearby globular cluster, NGC 6397. The next section describes the most important characteristic of NGC 6397 and the previous studies done regarding its compact binary population.

1.4.2 NGC 6397

NGC 6397 is the closest (2.4 kpc) core collapse[4] globular cluster (Harris, 1996; McLaughlin & van der Marel, 2005). The center of the cluster is located at RA(J2000): $17^h\,40^m\,42.09^s$ and Dec(J2000): $-53^\circ\,40'\,27.6$" (Harris, 1996). Due to its proximity NGC 6397 have been extensively studied in different wavelengths. The observation by Cool et al. (1993) with the ROSAT instrument was the first one to detect X-rays sources in NGC 6397. This was followed by a photometric study with the Hubble Space Telescope wide field and planetary camera confirming the first three CVs candidates in NGC 6397 (Cool et al., 1995). Since then observations with Chandra (Grindlay et al., 2001; Bogdanov et al., 2010) and more with Hubble (Taylor et al., 2001; Grindlay, 2006), both with the faint object spectrograph and with the advanced camera for surveys, have found a total of 15 CVs candidates (Cohn et al., 2010). From these current known 15 candidates only 4 have been spectroscopically confirmed (Grindlay et al., 1995; Edmonds et al., 1999), and the period is know for only two of them (Kaluzny & Thompson, 2003; Kaluzny et al., 2006).

In this work our goal is to exploit new data available from NGC 6397 and increase our understanding of CVs in globular clusters. We particularly try to extent the sample size of spectroscopically confirmed CVs and study their properties (e.g. period, mass and variability). In the next chapter we will discuss the nature of the observations and data used for the analysis.

[4]Core collapse are clusters showing a power-law slope in their surface brightness profile near the center due to the gravothermal instability (Antonov, 1962; Lynden-Bell & Wood, 1968; Lynden-Bell & Eggleton, 1980). In contrast to other isothermal sphere models showing a more flatten brightness profile in the center (e.g. King (1966))

Chapter 2: Observation and data reduction

2.1 VLT/MUSE

NGC 6397 was observed with the Multi Unit Spectroscopic Explorer (MUSE) at the Very Large Telescope (VLT) of the European Southern Observatory (ESO) at Paranal, Chile. MUSE is an integral field spectrograph (IFS). MUSE works by separating the full field of view ($1' \times 1'$) into 24 sub-fields (2.5" $\times$60"). Each of these 24 is them process by 24 identical but independent integral field units (IFU). Each IFU consists of an image slicer, an spectrograph and a CCD. Each IFU illuminates a 4k $\times$ 4k CCD after slicing the light into 48 slit-like slices (with size $\sim$ 15" $\times$ 0".2), and decomposing it via a volume phase holographic grating (Barden et al., 1998). The grating achieves a spectral resolution of 1750 at 4650 Å to 3750 at 9300 Å. The data from the 1152 slices is then reconstructed into a $1' \times 1'$ datacube (two spatial and one wavelength axis) with a 0".2 spatial resolution covering from 4750 Å to 9350 Å sampled at 1.25 Å (Bacon et al., 2010).

NGC 6397 was observed during the third commissioning period (ESO Programme ID 60.A-9100(C) Bacon et al. (2014)). The observation were taking from July 26nd to August 3rd, 2014. The observations covered the central part of NGC 6397 ($\sim 3'.5$ from the cluster center see fig 2.1). The dataset consists of 23 different pointings of MUSE with short exposure times ranging from 25-60 seconds. In total they obtained 127 exposures of the 23 different $1' \times 1'$ regions (see fig 2.1). This gives a total integration time of 95 minutes for all the observed part of the cluster.

2.2 Processed and Raw data

The primary goal of the MUSE observation of NGC 6397 was to create the first comprehensive Hertzsprung-Russell diagram with a sample of over 12 000 spectra (Husser et al., 2016). The large number of spectra obtained allow them to study the kinematics of the globular cluster with the goal to probe the presence of a central black hole in the cluster (Kamann et al., 2016). This data is publicly available thought the *MUSE Science Web Service*[1]. The website contains advanced science products such as reduced datacubes, source catalogs and software tools. For NGC 6397 it can be found the release of the spectra of the globular cluster NGC 6397 as published in the studies mentioned above (Husser et al. (2016) and Kamann et al. (2016)). They provide all the obtained spectra with a signal-to-noise ratio of five or larger, i.e. 14271 spectra in total. For our goal to study the CVs in the globular clusters the data wasn't enough as it mainly covers the range from main sequence to the tip of the red giant branch[2]. Our approach in this project was to work with the raw science data. The science data can be obtained from the ESO Science Archive Facility. As stated in the ESO Data Access Policy[3] all science data is made publicly available through the science archive after the proprietary period (normally one year after the data have been made available to the principal investigator) and all calibration data are public immediately after the observations.

[1] `http://muse-vlt.eu/science/`
[2] The red giant branch is
[3] `http://archive.eso.org/cms/eso-data-access-policy.html`

2.2.1 Data Reduction

The data was reduced with version 1.2.1 of the MUSE Instrument Pipeline Recipes[4](Weilbacher et al., 2012). The pipeline distribution kit includes several packages. The ones used for this work are the following:

- The Common Pipeline Library version 6.6 (McKay et al., 2004)
- The ESO Recipe Execution Tool (EsoRex)[5] version 3.12.

All the data reduction was done calling EsoRex to execute the MUSE DRS recipes from a bash (version 4.3.11) script[6] (alternative this can be done via the Python bindings (Streicher & Weilbacher, 2012)). We summarize the main steps to produce the fully reduced datacube from the raw science and calibration data download from the ESO Science Archive MUSE Query Form. The data reduction steps can be divided into two categories, pre-processing and post-processing. The pre-processing part includes all the necesarry claibration to remove the instrument signature on the exposures. The post-preoccessing then takes the resulting pixel table for each science observation and can resample them to create the datacube.

1. Calibration and pre-processing

   I **Bias substraction**: Bias subtraction was done by combining 10 different bias images into one master bias file. Each bias is part of the calibration files taken by ESO every night. A bias frame is dark image with no exposure time taken to account for the read out noise. (Recipe called *muse_bias*). For this an all subsequent steps we used a table of additional bad pixels of the CCDs created for the MUSE commission runs. This bad pixel table is distributed along with the MUSE pipeline files.

   II **Flat-fielding**: For the flat-field correction also 10 individual flat frames were combined into a master flat frame. The flat-field images are taking daily at the VLT as part of the standard calibration plan. The master flat contains the combined pixel values of the raw flat exposures. The purpose is to correct for uneven detector sensitivity. The recipe used was *muse_flat*. Besides the master flat, the recipe also produces a *trace table* containing polynomials defining the location of the slices on the CCD.

   III **Wavelenght calibration**: For the wavelenght calibration 15 different arc lamp exposures were used. These is 3 per lamp (Ne, Xe, HgCd lamps). The recipe used is *muse_wavecal*. It detects arc emission lines and determine the wavelength solution for each slice. The goal is to establish the pixel to wavelength equivalence with high precision.

   IV **Line Spread Function**: The line-spread function is calculated with the recipe *muse_lsf*. The lines spread function describes the broadening of spectral lines on a CCD. The recipe calculates this wavelenght dependent function from 15 arc lamp exposures, and the wavelength solution calculated in the step above.

[4]The MUSE pipeline can be found at `http://www.eso.org/sci/software/pipelines/muse/`

[5]EsoRex is written by the CPL group (Pipeline System Department) European Southern Observatory `http://www.eso.org/sci/software/cpl/esorex.html`

[6]All the configuration files for each of the called MUSE recipes used, the bash scripts, useful python (Python 2.7.6) scripts and other text files relevant for the data reduction can be found at `https://github.com/manuelmarcano22/muse2016`

V **Geometrical calibration**: In this step the recipe *muse_ geometry* can be used to determine where the field of view . This creates a geometry table. A geometry table comes with the standard MUSE pipeline package as a static calibration files. The geometry table prepared for the third commisioning period was used in reducing the data.

VI **Illumination Correction**: Flat-field with sky or twilight flats are taken weekly at the VLT. These are use to do large scale illumination correction. This is done calling the recipe *muse_ twilight*. For the illumination correction also an special purpose illumination flat field called ILLUM can be used as an input to the recipe. This are taken throught the observing night. We use the one taken closest in time to the science data.

2. Post-processing

I **Flux calibration**: In this step a flux response curve from a standard star exposure is created. The end produc of the *muse_ standard* are tables with the response curve as derived from standard star and also the telluric absorption as derived from standard star.

II **Sky substraction**: Was not done as it is only needed if the observed object fills the fiel of viw that reasonbale sky spectrum cannto be obtained on the obsergationitserf. The sky ubstractionos done dir. No sky

III **Astrometry**: Can compute astrometry solution, but the one shppied with the pipeline for the commisiing period was used.

IV **Combination** a full data cube is created from a single exposure, the sky background is removed and the flux calibration and the astrometric calibration, created in the preceding processing steps, are applied. In this step the cubes a sampled to a common value ($0".2 \times 0".2 \times 1.25\AA$) . The different for each region of the cluster where merged into a singe datacube and for the center dataxubes of indivial exposures were also created.

K-means from Creation fo the datacube from the above tables created telluric tables, reponese curve, sky cntinuum. Datacibe from single expisures of combining after correctly aligning them creatinan tabkle of ofset.

2.2.2 Spectra extration and analysis

The spectra substraction and analysis was carreid wtih QFits View and IRAF (Tody, 1986) Astropy (**?**)

Plit

This research made use of APLpy, an open-source plotting package for Python hosted at http://aplpy.github.com

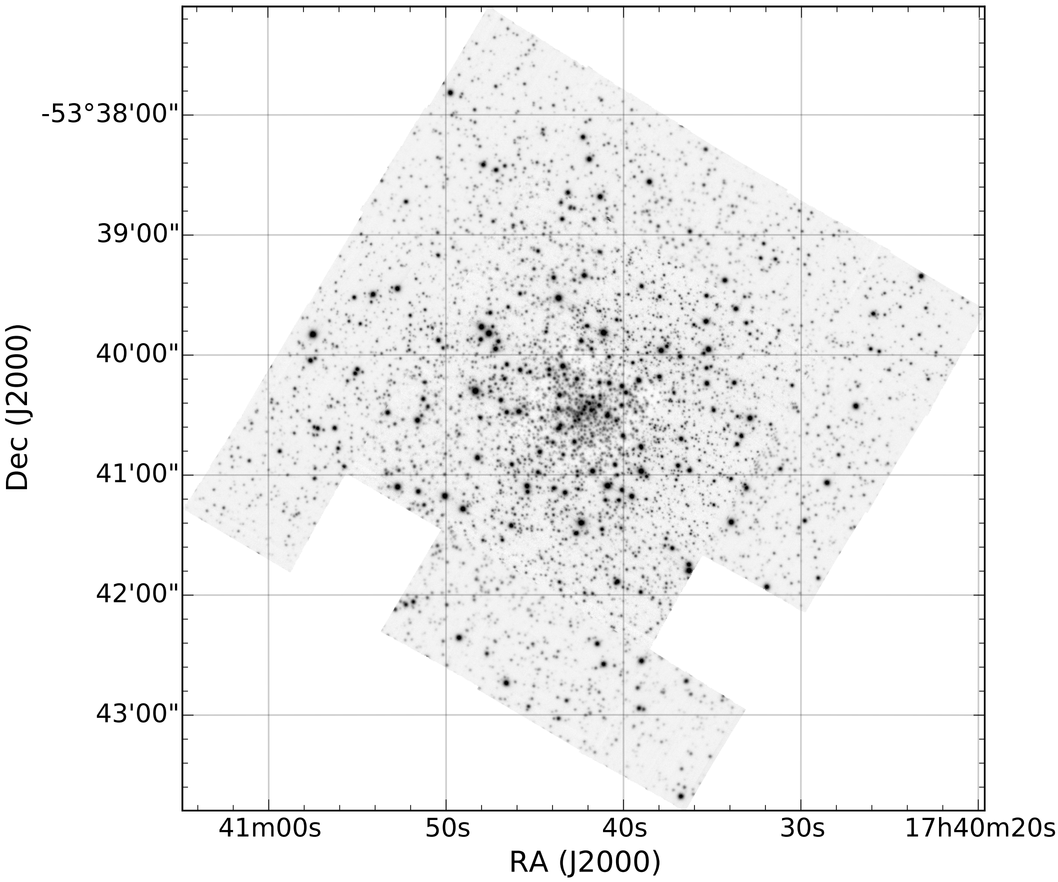

Figure 2.1: bfagagaga

Chapter 3: Results

3.1 Spectra

3.2 Variability

3.3 Mass ration

3.4 Radial Velocity

Bibliography

Antonov, V. A. 1962

Baade, W. & Zwicky, F. 1934, Proceedings of the National Academy of Sciences, 20, 259

Bacon, R., Accardo, M., Adjali, L., Anwand, H., Bauer, S., Biswas, I., Blaizot, J., Boudon, D., Brau-Nogue, S., Brinchmann, J., Caillier, P., Capoani, L., Carollo, C. M., Contini, T., Couderc, P., Daguisé, E., Deiries, S., Delabre, B., Dreizler, S., Dubois, J., Dupieux, M., Dupuy, C., Emsellem, E., Fechner, T., Fleischmann, A., François, M., Gallou, G., Gharsa, T., Glindemann, A., Gojak, D., Guiderdoni, B., Hansali, G., Hahn, T., Jarno, A., Kelz, A., Koehler, C., Kosmalski, J., Laurent, F., Le Floch, M., Lilly, S. J., Lizon, J.-L., Loupias, M., Manescau, A., Monstein, C., Nicklas, H., Olaya, J.-C., Pares, L., Pasquini, L., Pécontal-Rousset, A., Pelló, R., Petit, C., Popow, E., Reiss, R., Remillieux, A., Renault, E., Roth, M., Rupprecht, G., Serre, D., Schaye, J., Soucail, G., Steinmetz, M., Streicher, O., Stuik, R., Valentin, H., Vernet, J., Weilbacher, P., Wisotzki, L., & Yerle, N. 2010, in Proceedings of the SPIE, Vol. 7735, Ground-based and Airborne Instrumentation for Astronomy III, 773508

Bacon, R., Vernet, J., Borisova, E., Bouche, N., Brinchmann, J., Carollo, M., Carton, D., Caruana, J., Cerda, S., Contini, T., Franx, M., Girard, M., Guerou, A., Haddad, N., Hau, G., Herenz, C., Herrera, J. C., Husemann, B., Husser, T.-O., Jarno, A., Kamann, S., Krajnovic, D., Lilly, S., Mainieri, V., Martinsson, T., Palsa, R., Patricio, V., Pecontal, A., Pello, R., Piqueras, L., Richard, J., Sandin, C., Schroetter, I., Selman, F., Shirazi, M., Smette, A., Soto, K., Streicher, O., Urrutia, T., Weilbacher, P., Wisotzki, L., & Zins, G. 2014, The Messenger, 157, 13

Balman, S. 2012, Memorie della Societa Astronomica Italiana, 83, 585

Barden, S. C., Arns, J. A., & Colburn, W. S. 1998, in Proceedings of the SPIE, Vol. 3355, Optical Astronomical Instrumentation, ed. S. D'Odorico, 866–876

Beskin, V., Balogh, A., Falanga, M., & Treumann, R. 2015, Space Science Reviews, 191, 1

Bogdanov, S., Berg, M. v. d., Heinke, C. O., Cohn, H. N., Lugger, P. M., & Grindlay, J. E. 2010, The Astrophysical Journal, 709, 241

Brown, G., Lee, C.-H., Wijers, R., & Bethe, H. 2000, Physics Reports, 333-334, 471

Cannizzo, J. K. & Mattei, J. A. 1998, The Astrophysical Journal, 505, 344

Chandrasekhar, S. 1931, The Astrophysical Journal, 74, 81

Cohn, H. N., Lugger, P. M., Couch, S. M., Anderson, J., Cool, A. M., van den Berg, M., Bogdanov, S., Heinke, C. O., & Grindlay, J. E. 2010, The Astrophysical Journal, 722, 20

Cool, A. M., Grindlay, J. E., Cohn, H. N., Lugger, P. M., & Slavin, S. D. 1995, The Astrophysical Journal, 439, 695

Cool, A. M., Grindlay, J. E., Krockenberger, M., & Bailyn, C. D. 1993, The Astrophysical Journal Letters, 410, L103

Coppejans, D. L., Koerding, E. G., Miller-Jones, J. C. A., Rupen, M. P., Knigge, C., Sivakoff, G. R., & Groot, P. J. 2015, arXiv:1506.00003 [astro-ph], arXiv: 1506.00003

Cropper, M. 1990, Space Science Reviews, 54

de Boer, K. & Seggewiss, W. 2008, Stars and Stellar Evolution (EDP Sciences)

De Loore, C. W. H. & Doom, C. 1992, Astrophysics and Space Science Library, Vol. 179, Structure and Evolution of Single and Binary Stars (Dordrecht: Springer Netherlands)

Duncan, R. C. & Thompson, C. 1992, The Astrophysical Journal, 392, L9

Edmonds, P. D., Grindlay, J. E., Cool, A., Cohn, H., Lugger, P., & Bailyn, C. 1999, The Astrophysical Journal, 516, 250

Fowler, R. H. 1926, Monthly Notices of the Royal Astronomical Society, 87, 114

Frank, J., King, A., & Raine, D. J. 2002, Accretion Power in Astrophysics: Third Edition (Cambridge University Press)

Gehrz, R., Truran, J., Williams, R., & Starrfield, S. 1998, Publications of the Astronomical Society of the Pacific, 110, 3

Grindlay, J. E. 1999, in , eprint: arXiv:astro-ph/9901356, 377

Grindlay, J. E. 2006, Advances in Space Research, 38, 2923

Grindlay, J. E., Cool, A. M., Callanan, P. J., Bailyn, C. D., Cohn, H. N., & Lugger, P. M. 1995, The Astrophysical Journal Letters, 455, L47

Grindlay, J. E., Heinke, C. O., Edmonds, P. D., Murray, S. S., & Cool, A. M. 2001, The Astrophysical Journal Letters, 563, L53

Hamada, T. & Salpeter, E. E. 1961, The Astrophysical Journal, 134, 683

Harris, W. E. 1996, The Astronomical Journal, 112, 1487

Heger, A., Fryer, C. L., Woosley, S. E., Langer, N., & Hartmann, D. H. 2003, The Astrophysical Journal, 591, 288

Heuvel, V. D. & J, E. P. 1976, Structure and Evolution of Close Binary Systems, 73

Husser, T.-O., Kamann, S., Dreizler, S., Wendt, M., Wulff, N., Bacon, R., Wisotzki, L., Brinchmann, J., Weilbacher, P. M., Roth, M. M., & Monreal-Ibero, A. 2016, Astronomy and Astrophysics, 588, A148

Hut, P., McMillan, S., Goodman, J., Mateo, M., Phinney, E. S., Pryor, C., Richer, H. B., Verbunt, F., & Weinberg, M. 1992, Publications of the Astronomical Society of the Pacific, 104, 981

Ivanova, N., Belczynski, K., Fregeau, J. M., & Rasio, F. A. 2005, Monthly Notices of the Royal Astronomical Society, 358, 572

Ivanova, N., Heinke, C. O., Rasio, F. A., Taam, R. E., Belczynski, K., & Fregeau, J. 2006, Monthly Notices of the Royal Astronomical Society, 372, 1043

Kaluzny, J. & Thompson, I. B. 2003, The Astronomical Journal, 125, 2534

Kaluzny, J., Thompson, I. B., Krzeminski, W., & Schwarzenberg-Czerny, A. 2006, Monthly Notices of the Royal Astronomical Society, 365, 548

Kamann, S., Husser, T.-O., Brinchmann, J., Emsellem, E., Weilbacher, P. M., Wisotzki, L., Wendt, M., Krajnović, D., Roth, M. M., Bacon, R., & Dreizler, S. 2016, ArXiv e-prints, 1602, arXiv:1602.01643

Kepler, S. O. & Bradley, P. A. 1995, Baltic Astronomy, 4

King, I. R. 1966, The Astronomical Journal, 71, 64

Kinney, A. 1994, in Astronomical Society of the Pacific Conference Series, Vol. 54, The Physics of Active Galaxies, ed. G. V. Bicknell, M. A. Dopita, & P. J. Quinn, 61

Kippenhahn, R., Kohl, K., & Weigert, A. 1967, Zeitschrift fur Astrophysik, 66

Knigge, C. 2012, Memorie della Societa Astronomica Italiana, 83

Koester, D. & Chanmugam, G. 1990, Reports on Progress in Physics, 53, 837

Koester, D. & Weidermann, V. 1980, Astronomy and Astrophysics, 81

Kopal, Z. 1955, Annales d'Astrophysique, 18

—. 1959, Close binary systems (New York: Wiley)

Körding, E., Rupen, M., Knigge, C., Fender, R., Dhawan, V., Templeton, M., & Muxlow, T. 2008, Science, 320, 1318

Krzeminski, W. & Serkowski, K. 1977, The Astrophysical Journal, 216, L45

Kuulkers, E., Norton, A., Schwope, A., & Warner, B. 2006, in Compact stellar X-ray sources, 421–460

Lattimer, J. M. & Prakash, M. 2007, Physics Reports, 442, 109

Lubow, S. H. & Shu, F. H. 1975, The Astrophysical Journal, 198, 383

Lynden-Bell, D. & Eggleton, P. P. 1980, Monthly Notices of the Royal Astronomical Society, 191, 483

Lynden-Bell, D. & Pringle, J. E. 1974, Monthly Notices of the Royal Astronomical Society, 168, 603

Lynden-Bell, D. & Wood, R. 1968, Monthly Notices of the Royal Astronomical Society, 138, 495

McKay, D. J., Ballester, P., Banse, K., Izzo, C., Jung, Y., Kiesgen, M., Kornweibel, N., Lundin, L. K., Modigliani, A., Palsa, R. M., & Sabet, C. 2004, in , 444–452

McLaughlin, D. E. & van der Marel, R. P. 2005, The Astrophysical Journal Supplement Series, 161, 304

Meylan, G. & Heggie, D. C. 1997, Astronomy and Astrophysics Reviews, 8, 1

Osaki, Y. 1974, Publications of the Astronomical Society of Japan, 26, 429

Patterson, J. 1994, Publications of the Astronomical Society of the Pacific, 106, 209

Postnov, K. A. & Yungelson, L. R. 2014, Living Reviews in Relativity, 17

Prada Moroni, P. G. & Straniero, O. 2009, Astronomy and Astrophysics, 507, 1575

Reisenegger, A. 2005, in (AIP), 263–273

Rhoades, C. E. & Ruffini, R. 1974, Physical Review Letters, 32, 324

Schuerman, D. W. 1972, Astrophysics and Space Science, 19, 351

Shara, M. M. 1989, Publications of the Astronomical Society of the Pacific, 101, 5

Starrfield, S., Iliadis, C., & Hix, W. R. 2016, Publications of the Astronomical Society of the Pacific, 128, 051001

Streicher, O. & Weilbacher, P. M. 2012, Astronomical Data Analysis Software and Systems XXI, 461

Suh, I.-S. & Mathews, G. J. 2000, The Astrophysical Journal, 530, 949

Tapia, S. 1977, The Astrophysical Journal, 212, L125

Tauris, T. M. & van den Heuvel, E. P. J. 2006, in Compact stellar X-ray sources, 623–665

Taylor, J. M., Grindlay, J. E., Edmonds, P. D., & Cool, A. M. 2001, The Astrophysical Journal Letters, 553, L169

Tody, D. 1986, in Proceedings of the SPIE, Vol. 627, Instrumentation in astronomy VI, ed. D. L. Crawford, 733

Verbunt, F. 1982, Space Science Reviews, 32

Verbunt, F., Bunk, W. H., Ritter, H., & Pfeffermann, E. 1997, Astronomy and Astrophysics, 327

Warner, B. 2003, Cataclysmic Variable Stars (Cambridge University Press)

Weilbacher, P. M., Streicher, O., Urrutia, T., Jarno, A., Pécontal-Rousset, A., Bacon, R., & Böhm, P. 2012, 84510B

Wickramasinghe, D. T. & Ferrario, L. 2000, Publications of the Astronomical Society of the Pacific, 112, 873